Accepted Manuscript

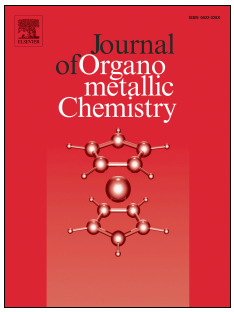

Ferrocenyl aza-dipyrromethene and aza-BODIPY: Synthesis and properties

Rekha Sharma, Ramesh Maragani, Rajneesh Misra

PII: S0022-328X(16)30467-3

DOI: 10.1016/j.jorganchem.2016.10.019

Reference: JOM 19663

To appear in: *Journal of Organometallic Chemistry*

Received Date: 8 September 2016

Revised Date: 13 October 2016

Accepted Date: 14 October 2016

Please cite this article as: R. Sharma, R. Maragani, R. Misra, Ferrocenyl aza-dipyrromethene and aza-BODIPY: Synthesis and properties, *Journal of Organometallic Chemistry* (2016), doi: 10.1016/j.jorganchem.2016.10.019.

Ferrocenyl Aza-dipyrromethene and Aza-BODIPY: Synthesis and Properties

Rekha Sharma, Ramesh Maragani and Rajneesh Misra*

Department of Chemistry, Indian Institute of Technology Indore, 453552

TOC

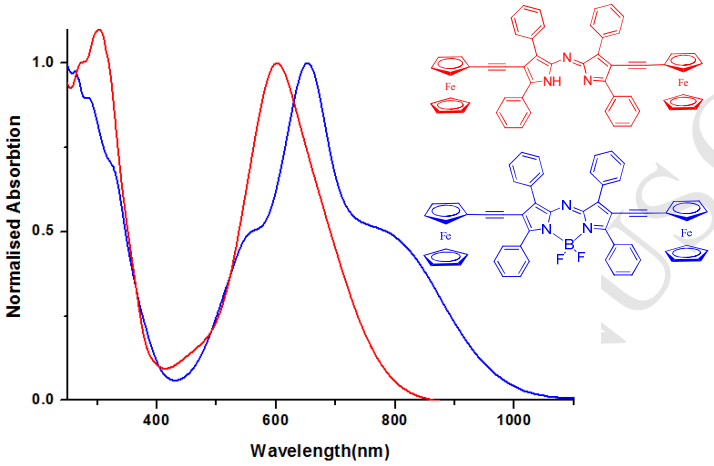

Abstract

A series of ferrocenyl substituted tetraphenylazadipyrromethane and Aza-BODIPY were designed and synthesized by the Pd-catalyzed Sonogashira cross-coupling reaction. The effect of the pyrrolic substituents on photophysical and electrochemical properties was explored. The results show substantial electronic communication between the ferrocene unit, and Aza-BODIPY core. The aza-dipyromethane and aza-BODIPY **3–6** are non-emissive in nature and their absorption maxima exhibit red shifted absorption compared to unsubstituted azabodipy. The computational calculation on Aza-BODIPY **5** and **6** was performed**,** which reveals that electron density transfers from ferrocene (donor) to azabodipy (acceptor) core and the photophysical properties are in good agreement with the computational data.

Introduction:

Aza-BODIPY dyes have received substantial attention of the scientific community due to their remarkable spectral properties such as high molar extinction coefficient and large fluorescence quantum yields.[1-2] These dyes have been extensively used in development of sensors, as near-

infrared absorbers and as a sensitizers in photodynamic therapy.[3-4] Aza-BODIPYs are structural analogues of BODIPYs with a nitrogen at 8- position instead of the carbon. These dyes exhibit red shifted absorption and emission bands compared to BODIPYs.[5] Several strategies have been explored to tune the photonic properties of Aza-BODIPY core including (a) coordination by BF_2,[6-8] (b) extending the conjugation through phenyl rings,[9-10] (c) restricting the conformation of Aza-BODIPY core,[11] and (d) replacing the phenyl rings with thiophene rings. [12-14]

Our group has explored BODIPYs, functionalized at the *meso*-position, as well as at the pyrrolic position.[15] The electron withdrawing Aza-BODIPY core is an important building block in a variety of donor–acceptor molecular systems, which enhances the charge transfer and lowers the HOMO-LUMO gap. This encouraged us to explore the Aza-BODIPY core and effect of the pyrrolic substituents on photophysical and electrochemical properties of these molecular systems.

Ferrocene is undoubtedly a strong electron donor.[17] The ferrocenyl derivatives are thermally and photochemically stable.[18] There are few reports where the ferrocenyl derivatives are connected to the Aza-BODIPY core via spacer at di ▪erent positions (Chart 1).[3b,19-21] To the best of our knowledge, there are no reports available on Aza-BODIPY dyes with ferrocene groups connected through pyrrolic position. Hence, in the context of our research on the ferrocenyl functionalized systems, we have attached the ferrocenyl group to one of the pyrrolic ring and both the pyrrolic rings of the tetraphenylazadipyrromethane and Aza-BODIPY respectively. The photophysical and electrochemical properties of all new compounds were studied and DFT calculations were performed to optimise the geometry and study the frontier molecular orbitals.

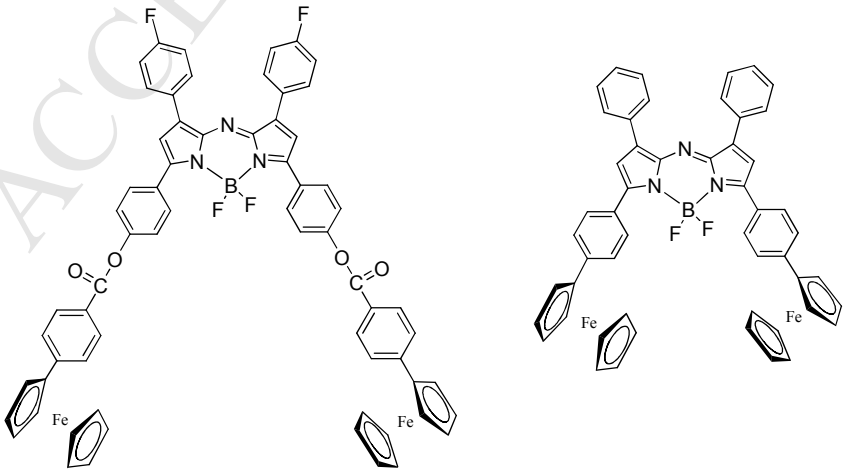

Chart **1**. Structures of reported Ferrocenyl Aza-BODIPY dyes

Results and discussion:

The synthesis of the ferrocenyl substituted tetraphenylazadipyrromethane and its BF_2 chelates **3–6** are shown in Scheme 2. The ferrocenyl substituted tetraphenylazadipyrromethane and Aza-BODIPY were synthesized in moderate yield by the Pd-catalyzed Sonogashira cross-coupling reaction of iodinated Aza-BODIPY(2) with the ethynyl ferrocene.

The iodinated Aza-BODIPY **2** was synthesized by four step reaction sequence starting from Aldol condensation reaction between benzaldehyde and acetophenone which resulted chalcone.[22] The addition of nitromethane to the chalcone in the presence of diethylamine resulted the nitro compound in 75–80% yield.[23] The nitro compound and ammonium acetate were boiled at reflux in ethanol under an argon atmosphere to obtain Aza-dipyrromethane.[23] The Aza-dipyrromethane precipitated during the reaction was filtered, recrystallized and used in next step without further purification. Aza-dipyrromethene was subsequently converted into the Aza-BODIPY derivatives by heating with trifluoroboron etherate and triethylamine in toluene. The iodination of Aza-BODIPY derivative was achieved using N-iodosuccinimide (NIS) in a mixture of $CHCl_3$ and acetic acid (3:1) in 80% yield (Scheme 1).[23]

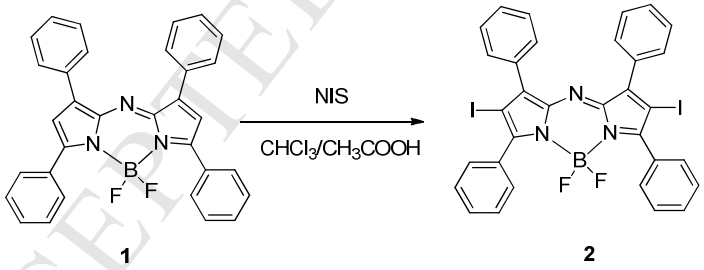

Scheme 1. Synthesis of iodinated Aza-BODIPY.

The Sonogashira coupling reaction of iodo Aza-BODIPY **2** with ethynylferrocene resulted in monosubstituted **3** and di-substituted ferrocenyl azapyromethanes **4**. It was noted that, contrarily to C-Bodipy analogues, the Pd-catalyzed cross coupling reaction resulted in the loss of a BF_2 fragment.[14,24] This was also confirmed by ^{19}F NMR. The monosubstituted and di-substituted ferrocenyl azapyromethanes were difficult to purify. So, first washing with cold methanol and diethyl ether removed most impurities,[25] including the monosubstituted product, followed by

column chromatography and recrystallization afforded pure ferrocenyl azapyromethanes **3** and **4**. The ferrocenyl aza-pyromethanes **3** and **4** were also well characterized by ^{1}H NMR, ^{13}C NMR and high-resolution mass spectrometry (HRMS) techniques. The ferrocenyl aza-pyromethanes **3** and **4** were again treated with trifluoroboron etherate in presence of diisopropylamine and dichloromethane to afford the ferrocenyl substituted Aza-BODIPY **5** and **6** (Scheme 2).

The BF_2 chelates were purified by column chromatography using 1:1 DCM/hexane which resulted purple-blue ferrocenyl substituted Aza-BODIPY **5** and **6**. The ferrocenyl substituted aza-BODIPY **5** and **6** were well characterized by NMR (^{1}H, ^{13}C, ^{11}B and ^{19}F) analysis and by high-resolution mass spectrometry (HRMS) (see Figures S5-S19, Supporting Information).

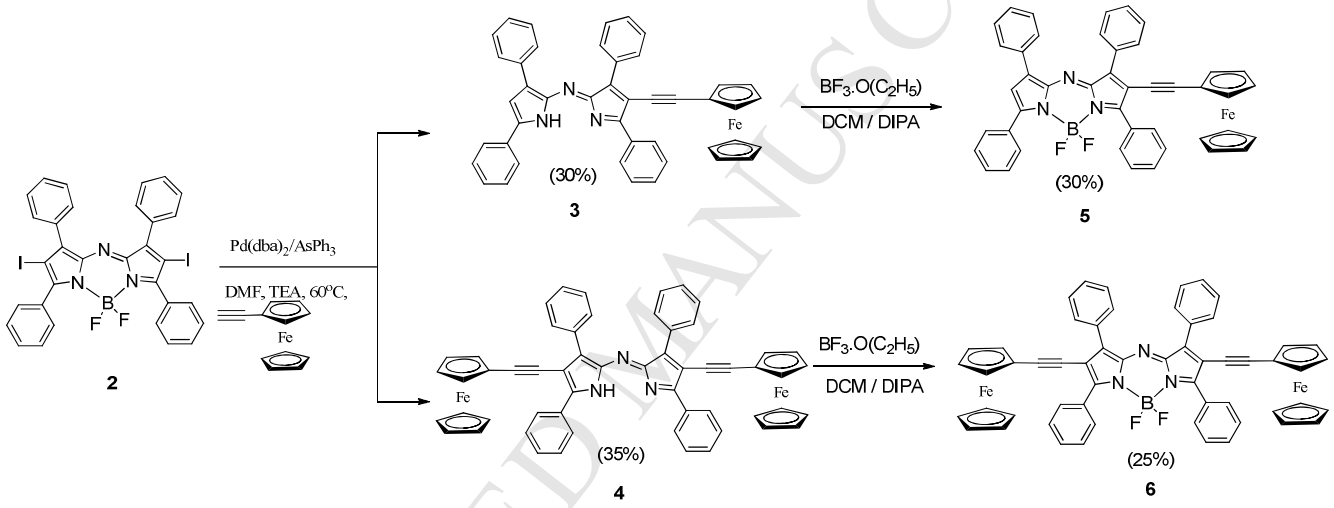

Scheme 2. Synthetic route for Ferrocenyl Aza-dipyrromethene and Aza-BODIPY **3–6**.

The ^{1}H NMR peaks for Aza-BODIPY **5** and **6** were shifted upfield compared with ferrocenyl aza-pyromethanes **3** and **4**. The ^{11}B NMR spectra of compounds **5** and **6** showed a triplet at δ = 0.70 and 0.80 ppm, respectively, which corresponds to the tetracoordinate boron center. The ^{19}F NMR signals of **5** and **6** were observed as a quartet due to the tetracoordinate boron atom at –131.50 and –131.05 ppm, respectively.[10b]

Photophysical properties

The electronic absorption spectra of the ferrocenyl substituted tetraphenylazadipyrromethane and Aza-BODIPY were recorded in chloroform at room temperature (Figure **1**), and data are listed in Table **1**. The absorption spectra of the ferrocenyl substituted tetraphenylazadipyrro methane and Aza-BODIPY exhibit two intense peaks, one in the UV region and another in the visible region with high extinction coefficient.

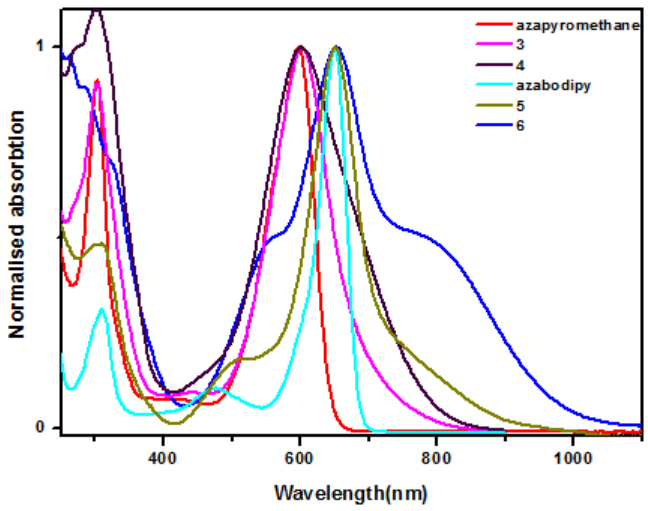

Figure 1: Electronic absorption spectra of the azapyromethane and azabodipy **3–6** at 1.0 × 10^{-5} M, recorded in chloroform.

The ferrocenyl tetraphenylazadipyrromethane **3** and **4** exhibit absorption maxima at 602 nm. The BF_2 coordination of ferrocenyl tetraphenylazadipyrromethane **3** and **4** results in a bathochromic shift of around 50 nm which is attributed to the extended conjugation. The ferrocenyl Aza-BODIPY **6** exhibit a shoulder band at 800 nm which is an intramolecular charge transfer from the ferrocenes to the Aza-BODIPY core.[26]

The ferrocenyl tetraphenylazadipyrromethane and Aza-BODIPY **3–6** are non emissive in nature due to the fast non-radiative deactivation of the excited state with intramolecular charge transfer.[27-28]

Electrochemistry

The electrochemical behavior of the ferrocenyl substituted tetraphenylazadipyrromethane and Aza-BODIPY (**3–6**) were investigated by the cyclic voltammetric analysis in anhydrous dichloromethane solution at room temperature using tetrabutylammoniumhexafluorophosphate ($TBAPF_6$) as a supporting electrolyte. The electrochemical data are listed in Table **1**, and the representative cyclic voltammogram of Aza-BODIPY **6** is shown in Figure **2**. The cyclic voltammograms of the Aza-BODIPY **3–5** can be found in the ESI section. All potentials are corrected to be referenced against FcH/FcH^+, as required by IUPAC.[29]

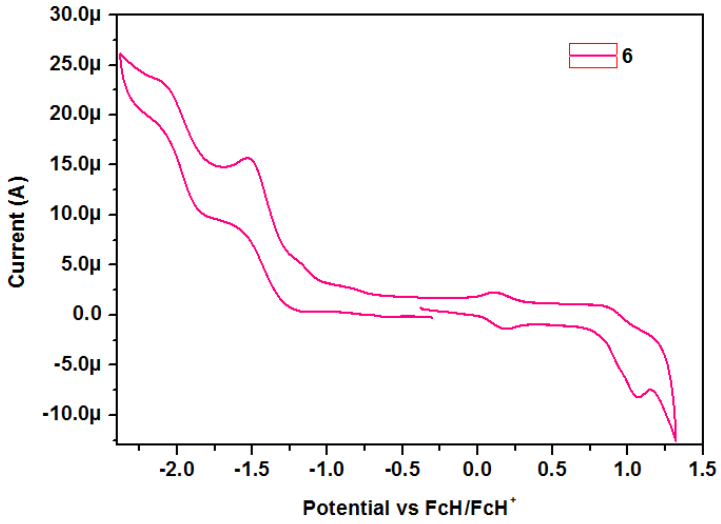

Figure 2: Cyclic voltammogram of 1.0×10^{-4} M solutions of Aza-BODIPY **6** in CH_2Cl_2 containing 0.1M Bu_4NPF_6 as supporting electrolyte, recorded at a scan speed of 100 mVs^{-1}.

The cylic voltammogram of the ferrocenyl substituted tetraphenylazadipyrromethane and Aza-BODIPY (**3–6**) show two reversible reduction peaks, one reversible oxidation peak (ferrocene/ferrocenium) and one irreversible oxidation peak. The ferrocene based reversible oxidation wave for tetraphenylazadipyrromethane and Aza-BODIPY (**3–6**) was observed at $E_{1/2}$ = 0.12–0.14 V. The ferrocenyl moieties in the tetraphenylazadipyrromethane and Aza-BODIPY (**3–6**) show higher oxidation potential compared to the free ferrocene. This confirms substantial electronic communication between ferrocene and Aza-BODIPY core. The second oxidation becomes easier in ferrocenyl tetraphenylazadipyrromethane and Aza-BODIPY (**3–6**) than unsubstituted azadipyrromethane and Aza-BODIPY.

The reduction of ferrocenyl tetraphenylazadipyrromethane and Aza-BODIPY becomes harder than unsubstituted azadipyrromethane and Aza-BODIPY. The mono ferrocenyl tetraphenylazadipyrromethane **3** shows two quasi reversible reduction peaks at $E_{1/2}$ = -1.18 – -1.51 V and diferrocenyl tetraphenylazadipyrromethane **4** shows at -1.56 and -2.18 V. The ferrocenyl Aza-BODIPYs **5** and **6** show multiple quasi reversible reduction peaks in the range of -0.8 – -2.07 V.

Table 1. Photophysical and electrochemical data of ferrocenyl tetraphenylazadipyrromethane and Aza-BODIPY **3–6.**

Compound	Photophysical data[a]	Electro-chemical data[b]	
	$\lambda_{max,}$ [nm] (ε[Lmol–cm^{-1}])	E_{ox}(V)	E_{red}(V)
Ferrocene	-	0.00	-
Azapyromethane	596 (68000)	0.98 1.86	-1.09 -1.41
3	602 (65000)	0.12 1.02	-1.18 -1.51
4	602 (66000)	0.13 1.03	-1.56 -2.18
Azabodipy	650 (79000)	1.10 1.44	-0.70 -1.53 -2.03
5	651 (67000)	0.13 1.09	-0.80 -1.47 -2.02
6	653 (70000)	0.14 1.06	-1.51 -2.07

[a] Measured in chloroform at 1.0×10^{-5} M concentration. [b]Recorded by cyclic voltammetry using 1.0×10^{-4} M solutions of **3—6**, containing 0.1 M solution of Bu_4NPF_6 in DCM at 100 mVs^{-1} scan rate, *vs* FcH/FCH^+ electrode.

Computational calculations

The structural and electronic properties of the ferrocenyl substituted Aza-BODIPYs (**5** and **6**) were explored by means of Computational calculations. The Aza-BODIPYs **5** and **6** were optimized by using Gaussian 09W program at the B3LYP/6-31G** level for C, H, N and LANL2DZ for Fe.[30-32]

The optimized structure of ferrocenyl substituted Aza-BODIPY **6** show eclipsed conformation of cyclopentadienyl rings of the ferrocenyl groups (Figure **3**). The dihedral angle in unsubstituted Aza-BODIPY, between phenyl ring (C28, 29, 32, 34, 30, 27) and Aza-BODIPY core was found 36.67°, while in ferrocenyl substituted Aza-BODIPY **6** the dihedral angle between phenyl ring and Aza-BODIPY core is 23.10° (Figure **S3**).

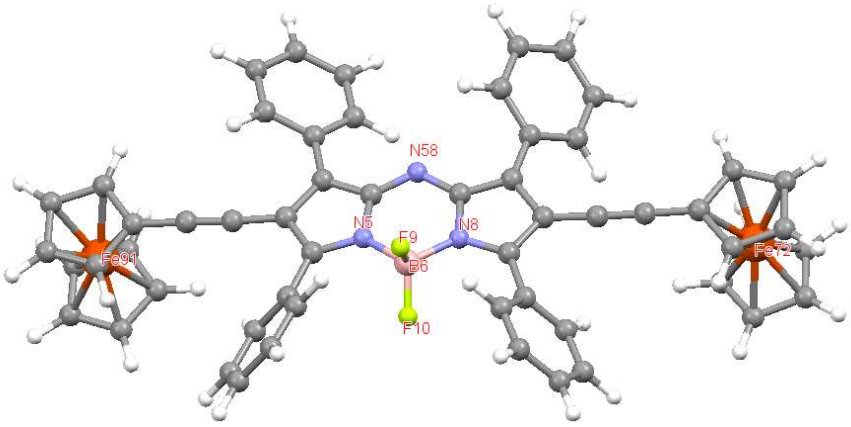

Figure 3. The DFT optimized structure of ferrocenyl substituted Aza-BODIPY **6** using B3LYP level. The 6-31G** basis set for C, N, H and LANL2DZ for Fe

In order to understand the photophysical properties of azabodipy the time dependent density functional calculation (TD-DFT) was carried out using B3LYP method for Aza-BODIPY and ferrocenyl substituted Aza-BODIPY **5** and **6** in chloroform solvent using polarized continuum model (CPCM) of Gaussian 09 software. The experimental and computational (TD-DFT: B3LYP) UV-vis absorption spectra are shown in Figure **S4**. The strong absorption band calculated at B3LYP level is 588 nm for Aza-BODIPY and 616 nm for ferrocenyl substituted Aza-BODIPY **5** and **6**. The experimental values for Aza-BODIPY and ferrocenyl Aza-BODIPY **5** and **6** are 650 and 651 nm respectively. The experimental values are in good agreement with theoretical values.

The predicted vertical transitions and oscillator strengths in ferrocenyl substituted Aza-BODIPY **5** and **6** are listed in Table **2**. In ferrocenyl substituted Aza-BODIPY **5** the transition is dominated by HOMO→LUMO+1 transition 68% and oscillator strength is 0.4908. In Aza-BODIPY **6**, the HOMO→LUMO+1 transition contribute to the lowest excited state by 44%, which belongs to π-π* transition. The Aza-BODIPY **6** shows one more contribution (32%) between HOMO-1→LUMO, which corresponding to the ICT transition at 779 nm as shown in Figure **4**.

Table 2. Computed vertical transition energies and their Oscillator strengths (*f*) and major contributions for the Aza-BODIPY **5** and **6**

	TD-DFT/ B3LYP (DCM)		
	λ_{max}	f^a	**Major contribution** (%)
Aza Bodipy	588 nm	0.8351	HOMO→LUMO (100%)
	616 nm	0.4908	HOMO → LUMO+1(68%)
5	624 nm	0.2701	HOMO-2→LUMO (56%)
	616 nm	0.4178	HOMO →LUMO+1 (44%)
6	779 nm	0.1431	HOMO−1→LUMO (32%)

[a]f is Oscillator strengths

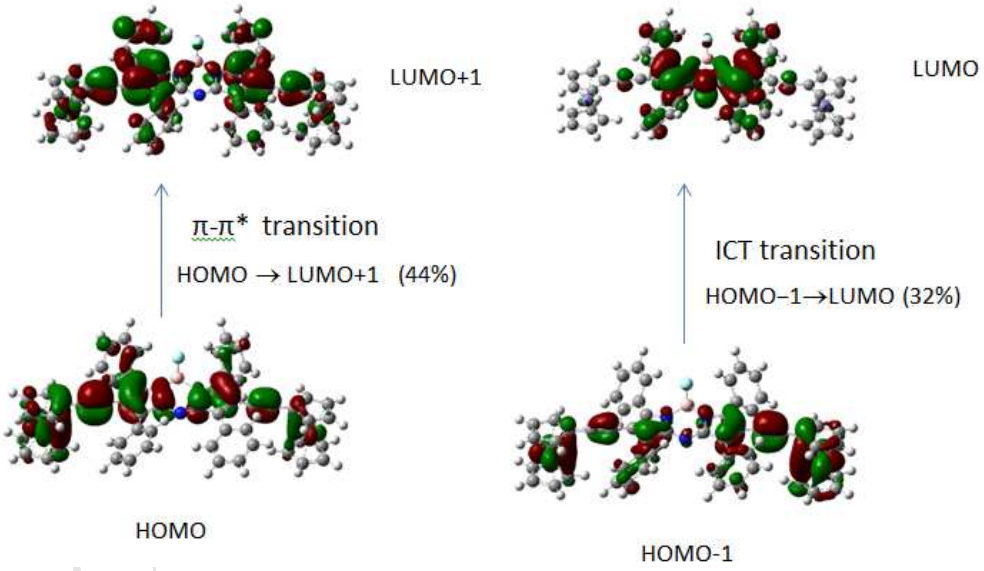

Figure 4. The major transitions in Aza-BODIPY **6**

The Figure **5** shows the electron density distribution of the HOMO and LUMO of the ferrocenyl substituted Aza-BODIPY **5** and **6** obtained using TD-DFT/B3LYP method. The electron densities of HOMOs in the Aza-BODIPY **5** and **6** are delocalized over the ferrocenyl and Aza-BODIPY core, whereas the LUMOs are located only on the Aza-BODIPY core. The HOMO-LUMO gap is lower in ferrocenyl substituted Aza-BODIPY **6** as compared to the Aza-BODIPY and monosubstituted Aza-BODIPY **5**. These results reveal that by increasing conjugation the

electronic communication increases in Aza-BODIPY **6** and band gap decreases. The comparsion of optical band gap with theoretical band gap are listed in the Table S1.

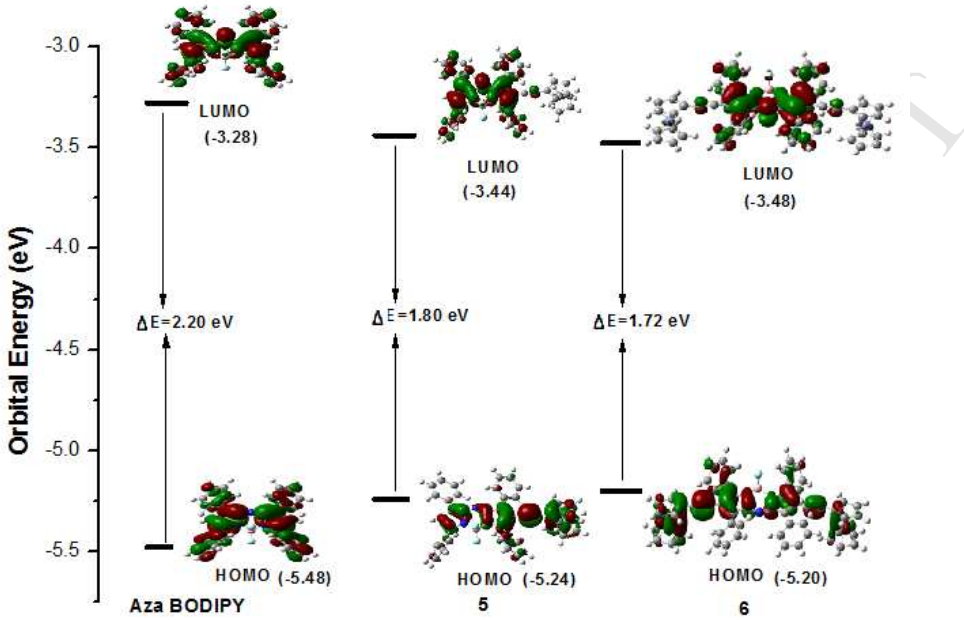

Figure 5. The energy level diagram of the frontier molecular orbitals of the ferrocenyl substituted Aza-BODIPY **5** and **6** calculated using B3LYP level of TD-DFT theory.

Conclusions

In summary, we have synthesized ferrocenyl substituted tetraphenylazadipyrromethane and Aza-BODIPY by the Pd-catalyzed Sonogashira cross-coupling reaction. The UV-visible absorption, electrochemical and computational studies of these molecules show good electronic interaction. The absorption maxima of Aza-BODIPY **5** and **6** show considerable red shift compared to the ferrocenyl substituted tetraphenylazadipyrromethane. The DFT and TD-DFT results reveal that electron density transfers from ferrocene (donor) to azabodipy (acceptor) core. The computational calculations of Aza-BODIPY **5** and **6** are in good agreement with the experimental data. The Aza-BODIPYs reported here are potential candidates for biological imaging and organic photovoltaic applications and their detailed study is currently on going in our laboratory.

Experimental section:

General: Chemicals were used as received unless otherwise indicated. All oxygen or moisture sensitive reactions were performed under nitrogen/argon atmosphere using standard schlenk method. Triethylamine (TEA) was received from commercial source, and distilled on KOH prior to use. ^{1}H NMR (400 MHz), and ^{13}C NMR (100MHz) spectra were recorded on the Bruker Avance (III) 400 MHz, using $CDCl_3$ as solvent. Tetramethylsilane (TMS) was used as reference for recording ^{1}H (of residual proton; δ = 7.26 ppm), and ^{13}C (δ = 77.0 ppm) spectra in $CDCl_3$. UV-visible absorption spectra of all compounds in chlorofom were recorded on a Carry-100 Bio UV-visible Spectrophotometer. Cyclic voltamograms (CVs) were recorded on a CHI620D electrochemical analyzer using glassy carbon as a working electrode, Pt wire as the counter electrode, and Ag/Ag^{+} as the reference electrode. HRMS was recorded on Brucker-Daltonics, micrO TOF-Q II mass spectrometer.

Synthesis and Characterization

The ethynyl ferrocene was purchased from Sigma-Aldrich, and iodo Aza-BODIPY was synthesized according to known methods.

Synthesis of ferrocenyl aza-pyromethanes and aza-BODIPY:

Iodo azabodipy (100 mg, 0.13 mmol) was stirred together with $Pd(dba)_2$ (40 mg, 0.05 mmol) and $AsPh_3$ (115 mg) in degassed DMF (15 mL) and triethyl amine (15ml) for 30 min at room temperature before the ethynyl ferrocene (2.5 equivalent) was added. The mixture was heated at 80 ºC for 48 h. The solvent was removed; the remaining residue was suspended in water (50 mL) and extracted with EtOAc (3 x 20 mL). The combined organic layers were dried ($MgSO_4$) and concentrated in vacuum. The resulting crude product was purified by column chromatography on silica gel eluting with CH_2Cl_2/hexane (2:3).

Aza-BODIPY BF_2.

Ferrocenyl substituted aza-pyromethanes (33 mg, 0.044 mmol) was dissolved in dry dichloromethane (DCM) (15 mL) and 100 mL of diisopropylethylamine was added. Trifluoroboron etherate (200 mL) was added to the mixture via a syringe. The reaction mixture was stirred overnight at room temperature. The solution was washed with distilled water (50 mL) and dried over anhydrous $Mg(SO4)_2$. The solvent was rotary evaporated to obtain a dark blue solid. The product was further purified by column chromatography on silica gel with 1: 1 DCM/hexanes to afford a purple-blue solid.

Ferrocenyl aza-pyromethanes 3:

purple solid (Yield 30%).^{1}H NMR (400 MHz, $CDCl_3$): δ (ppm) 8.44 (d, 2H, *J* = 7.66 Hz), 8.21 (d, 2H, *J* = 7.66 Hz), 8.08 (d, 2H, *J* = 7.66 Hz), 7.84 (d, 2H, *J* = 7.66 Hz), 7.61-7.30 (m, 13H), 7.13 (s, 1H), 4.52 (s, 2H), 4.29 (s, 2H), 4,25-4.20 (m, 5H).

^{13}C NMR (100 MHz, $CDCl_3$): δ = 161.49, 153.61, 148.22, 145.12, 144.96, 139.67, 133.66, 133.30, 132.97, 131.22, 130.53, 130.43, 129.62, 129.24, 128.86, 128.59, 128.31, 128.25, 127.91, 127.71, 125.92, 115.28, 111.84, 98.97, 81.85, 71.28, 69.95, 69.12, 65.52. HRMS (ESI) m/z, calcd for M^+H ($C_{44}H_{31}FeN_3$): 658.1941; found: 658.1784.

Ferrocenyl aza-pyromethanes 4:

Blue solid (Yield 35%). ^{1}H NMR (400 MHz, $CDCl_3$): δ (ppm) 8.26 (d, 4H, *J* = 7.79 Hz), 8.14 (d, 4H, *J* = 7.79 Hz), 7.52-7.28 (m, 12H), 4,45 (s, 4H), 4.21 (s, 4H), 4.15 (s, 10H).

^{13}C NMR (100 MHz, $CDCl_3$): δ = 154.16, 148.19, 141.17, 138.26, 131.80, 131.26, 129.31, 129.22, 127.72, 127.16, 127.00, 126.69, 114.89, 113.04, 111.27, 96.70, 80.41, 70.24, 68.90, 68.03, 64.54, 52.30. HRMS (ESI) m/z, calcd for M^+ H ($C_{56}H_{38}Fe_2N_3$): 865.1840; found: 865.1882.

Ferrocenyl aza-BODIPY 5:

Purple solid (Yield 30%). ^{1}H NMR (400 MHz, $CDCl_3$): δ (ppm) 8.25 (d, 2H, *J* = 7.50 Hz), 8.10-7.98 (m, 6H), 7.56-7.40 (m, 12H), 4.38 (s, 2H), 4.21 (s, 2H), 4.08 (m, 5H).

^{13}C NMR (100 MHz, $CDCl_3$): δ = 160.68, 160.56, 146.39, 144.67, 144.00, 142.12, 132.05, 132.01, 131.34, 131.19, 130.66, 130.44, 129.73, 129.62, 129.34, 128.66, 128.11, 127.82, 119.24, 114.96, 97.04, 79.39, 71.29, 69.94, 69.04, 64.91, 29.69 . ^{11}B: δ =0.70 (t), ^{19}F: δ = -131.48. HRMS (ESI) m/z, calcd for M^+ H ($C_{44}H_{30}BF_2FeN_3$): 705. 1853; found: 705.1886.

Ferrocenyl aza-BODIPY 6:

Blue solid (Yield 25%). ^{1}H NMR (400 MHz, $CDCl_3$): δ (ppm) 8.26 (d, 4H, *J* = 7.79 Hz), 7.99 (d, 4H, *J* = 7.79 Hz), 7.54-7.41 (m, 12H), 4.37 (s, 4H), 4.20 (s, 4H), 4.07 (s, 10H).

^{11}B: δ =0.70 (t), ^{19}F: δ = -131.48. HRMS (ESI) m/z, calcd for M^+ H ($C_{56}H_{37}BF_2Fe_2N_3$): 913.1832; found: 913.1946.

Acknowledgements

The work was supported by DST and CSIR, Govt. of India, New Delhi. We gratefully acknowledge Sophisticated Instrumentation Centre (SIC), IIT Indore.

Notes and references

*Department of Chemistry, Indian Institute of Technology Indore, 452017, India. Fax: +91 731 2361 482; Tel: +91 731 2438 710 * E-mail rajneeshmisra@iiti.ac.in*

†Electronic Supplementary Information (ESI) available: General experimental methods, and copies of ^{1}H NMR, and HRMS spectra of all new compounds.

References:

1. (a) A. Gorman, J. Killoran, C. O'Shea, T. Kenna, William M. Gallagher, and D. O'Shea J. Am. Chem. Soc., 126, (2004), 10619-10631. (b) H. Lu, S. Shimizu, J. Mack, Z. Shen, and N. Kobayashi, Chem. Asian J., 6, (2011), 1026 – 1037. (C) El-Khouly, S. Fukuzumi, F. D'Souza, Chem phys chem. (2014), 30-47.

2. (a) R. Gresser, H. Hartmann , M. Wrackmeyer, K. Leo, and M. Riede, Tetrahedron, 67, (2011), 7148-715. (b) J. Zhao, K. Xu, W. Yang, Z. Wang and F. Zhong Chem. Soc. Rev.**,** 44 (2015), 8904-8939. (C) S. Guo, L. Ma, J. Zhao, B. Küçüköz, A. Karatay, M. Hayvali, H. G. Yaglioglu and A. Elmali, Chem. Sci.**,** 5, (2014), 489-500.

3. (a) J. Killoran, L. Allen, J. F. Gallagher, W. M. Gallagher and D. F. O'Shea, Chem. Commun., (2002), 1862–1863. (b) A. N. Amin, M. E. Khouly, N. K. Subbaiyan, M. E. Zandler, M. Supur, S. Fukuzumi, and F. D'Souza, J. Phys. Chem. A, 115, (2011), 9810–9819.

4. A. D. Quartarolo, N. Russo, and E. Sicilia, Chem. Eur. J., 12, (2006), 6797 – 6803.

5. S. Kumar, H. B. Gobeze, T. Chatterjee, F. D'Souza, and M. Ravikanth, J. Phys. Chem. A 119, (2015), 8338−8348.

6. S. A. Berhe, M. T. Rodriguez, E. Park, V. N. Nesterov, H. Pan, and W. J. Youngblood, Inorg. Chem., 53, (2014), 2346−2348.

7. V. Bandi, H. B. Gobeze, V. N. Nesterov, P. A. Karrb and F. D'Souza, Phys. Chem. Chem. Phys., 16, (2014), 25537−25547.

8. N. Deligonul, A. R. Browne, J. A. Golen, A. L. Rheingold, and T. G. Gray, Organometallics, 2014, **33**, 637−643.

9. (a) H. Lu, S. Shimizu, J. Mack, Z. Shen, and N. Kobayashi, Chem. Asian J., 6, (2011), 1026 – 1037. (b) S. Shimizu, T. Iino, Y. Arakib and N. Kobayashi, Chem. Commun., 49, (2013), 1621-1623.

10. (a) X. Ma, X. Mao, S. Zhang, X. Huang, Y. Cheng and C. Zhu, Polym. Chem., 4, (2013), 520–527. (b) W. Senevirathna, J. Liao, Z. Mao, J. Gu, M. Porter, C. Wang, R. Fernando and G. Sauve, J. Mater. Chem. A, 3, (2015), 4203–4214.

11. W. Senevirathna and G. Sauve, J. Mater. Chem. C, 1, (2013), 6684—6694.

12. (a) C. Cheng, N. Gao, C. Yu, Z. Wang, J. Wang, E. Hao, Y. Wei, X. Mu, Y. Tian, C. Ran, and L. Jiao, Org. Lett., 17, 2015, 278−281 (b) X. Zhang, H. Yu, and Y. Xiao, J. Org. Chem. 77, (2012), 669−673. (c) C. Swamy , R. N. Priyanka, S. Mukherjee, and P. Thilagar, Eur. J. Inorg. Chem., 13, (2015), 2338–2344.

13. X. D. Jiang, Y. Fu, T. Zhang, W. Zhao, Tetrahedron Lett., 53, (2012), 5703–5706.

14. Q. Bellier, F. Dalier, E. Jeanneau, O. Maury and C. Andraud, New J. Chem., 36, (2012), 768–773.

15. (a) R. Misra, B. Dhokale, T. Jadhav and S. M. Mobin, Dalton Trans., 42, (2013), 13658–13666 (b) B. Dhokale, P. Gautam, S. M. Mobin and R. Misra, Dalton Trans., 42, (2013), 1512–1518. (c) J. Chen, M. Mizumura, H. Shinokubo and A. Osuka, Chem. Eur. J., 42, (2009), 5942–5949; (d) E. Y. Schmidt, B. A. Trofimov, A. I. Mikhaleva, N. V. Zorina, N. I. Protzuk, K. B. Petrushenko, I. A. Ushakov, M. Y. Dvorko, R. Meallet- Renault, G. Clavier, T. T. Vu, H. T. T. Tran and R. B. Pansu, Chem. Eur. J., 15, (2009), 5823–5830; (e) G. Ulrich, R. Ziessel and A. Harriman, Angew. Chem., Int. Ed., 47, (2008), 1184– 1201.

16. A. B. Nepomnyashchii, M. Broring, J. Ahrens, and A. J. Bard, J. Am. Chem. Soc., 133, (2011), 8633–8645.

17. (a) R. Misra, R. Sharma and S. M. Mobin, Dalton Trans., 43, (2014), 6891-6896 (b) P. Gautam, B. Dhokale, V. Shukla, P. C. Singh, K. S. Bindra and R. Misra, J. Photochem. photobio. A., 239, (2012), 24–27; (c) R. Maragani, T. Jadhav, S. M. Mobin and R. Misra, Tetrahedron, 68, (2012), 7302-7308; (d)) W. Y. Wong, K. Y. Ho, S. L. Ho, and Z. Lin, J. Organomet. Chem., 683, (2003), 341-353; (e) A. Auger, A. J. Muller and J. C. Swarts, Dalton Trans., (2007), 3623–3633.

18. (a) R. Misra, P. Gautam, T. Jadhav, and S. M. Mobin, J. Org. Chem., *78*, (2013), 4940-4948; (b) R. Misra, P. Gautam, and S. M. Mobin, J. Org. Chem., 78, (2013), 12440-12452 (c) R. Misra, T. Jadhav and S. M. Mobin, Dalton Trans., 42, (2013), 16614 (d) R. Sharma, P. Gautam, S. M. Mobin and R. Misra, Dalton Trans., 42, (2013), 5539-5545. (e) W. Y. Wong, G. L. Lu, K. H. Choi and Y. H. Guo, J. Organomet. Chem., 690, (2005), 177-186.

19. V. Bandi, M. Khouly, K. Ohkubo, V. N. Nesterov, M. E. Zandler, S. Fukuzumi, and F. D'Souza, J. Phys. Chem. C, 118, (2014), 2321−2332.

20. C. J. Ziegler, K. Chanawanno, A. Hasheminsasab, Y. V. Zatsikha, E. Maligaspe, and V. N. Nemykin, Inorg. Chem., 53, (2014), 4751–4755.

21. Y. V. Zatsikha, E. Maligaspe, A. A. Purchel, N. O. Didukh, Y. Wang, Y. P. Kovtun, D. A. Blank, and V. N. Nemykin, Inorg. Chem. 54, (2015), 7915−7928.

22. N. Adarsh, M. Shanmugasundaram, R. R. Avirah, and D. Ramaiah, Chem. Eur. J., 18, (2012), 12655 – 12662.

23. L. P. Jameson and S. V. Dzyuba, Bioorg. Med. Chem. Lett,. 23, (2013), 1732–1735.

24. (a) L. Gao, W. Senevirathna and G. Sauve, Org. Lett., 13, (2011), 5354. (b) Q. Bellier, S. Pegaz, C. Aronica, B. Le Guennic, C. Andraud and O. Maury, Org. Lett., 13, (2011), 22.

25. W. Senevirathna, J. Liao, Z. Mao, J. Gu, M. Porter, C. Wang, R. Fernando and G. Sauve, J. Mater. Chem. A, 3, (2015), 4203–4214.

26. (a)V. N. Nemykin, A. Y. Maximov and A. Y. Koposov, Organometallics, 26, (2007), 3138-3148; (b) B. Breiten, M. Jordan, D. Taura, M. Zalibera, M. Griesser, D. Confortin, C. Boudon, J. P. Gisselbrecht, W. B. Schweizer, G. Gescheidt and F. Diederich, J. Org. Chem., 78, (2013), 1760−1767.

27. (a) B. Dhokale, P. Gautam and R. Misra, Tetrahedron Lett., 78, (2012), 53, 2352–2354. (b) J. Rochford and M. T. P. Rooney, Inorg. Chem., 46, (2007), 7247. (c) M. R. Rao, K. V. Pavan Kumar and M. Ravikanth, J. Organomet. Chem., 695, (2010), 863-869.

28. (a) S. Fery-Forgues, and Delavaux-Nicot, J. Photochem. Photobio. A., 132, (2000), 137-159. (b) V. A. Nadtochenko, N. N. Denisov, V. Y. Gak, N. V. Abramova and N. M. Loim, Russ. Chem. Bull. 148, (1999), 1900. (c) S. Barlow and S. R. Marder, Chem. Commun., (2000), 1555-1562.

29. G. Gritzner and J. Kuta, Pure Appl. Chem., 56, (1984), 461.

30. (a) A. D. Becke, J. Chem. Phys., 98, (1993), 5648–5652; (b) C. T. Lee, W. T. Yang and R. G. Parr, Phys. Rev. B: Condens. Matter, 37, (1988), 785–789; (c) P. J. Hay and W. R. Wadt, *J.* Chem. Phys., 82, (1985), 270–283; (d) M. M. Francl, W. J. Pietro, W. J. Hehre, J. S. Binkley, M. S. Gordon, D. J. Defrees and D. J. A. Pople, J. Chem. Phys., 77, (1982), 3654–3665; (e) F. Ding, S. Chen and H. Wang, Materials, 3, (2010), 2668–2683.

31. (a) R. Maragani, P. Gautam, S. M. Mobin and R. Misra, Dalton Trans., 45, (2016), 4802–4809. (b) A. Pedone, J. Chem. Theory Comput., 9, (2013), 4087– 4096.

32. D. G. Gusev, Organometallics, 32, (2013), 4239–4243.